Open

Distinct differences in anterior chamber configuration and peripheral aberrations in negative dysphotopsia

Luc van Vught, BSc, Gregorius P.M. Luyten, MD, PhD, FEBOphth, Jan-Willem M. Beenakker, MSc, PhD

Purpose: To provide insights into the anatomical characteristics associated with negative dysphotopsia using quantitative clinical data.

Setting: Department of Ophthalmology, Leiden University Medical Center, Leiden, the Netherlands.

Design: Case-control study.

Methods: Anterior chamber tomography and peripheral aberrometry were measured in 27 pseudophakic patients with negative dysphotopsia and 30 pseudophakic control subjects. Based on these measurements, the total corneal power, anterior chamber depth, pupil location and diameter, iris tilt, and peripheral ocular wavefront up to 30 degrees eccentricity were compared between both groups. In addition, ray-tracing simulations using pseudophakic eye models were performed to establish a connection between these clinical measurements and current hypotheses on the etiology of negative dysphotopsia.

Results: Twenty-seven patients with negative dysphotopsia and 25 pseudophakic controls were included in the analysis. The patients with negative dysphotopsia had a smaller ($P = .03/P = <.01$) and more decentered ($P < .01$) pupil than that of the pseudophakic controls. In addition, an increased temporal-tilted iris ($P < .01$) and an asymmetric peripheral aberration profile were observed in patients with negative dysphotopsia, of which the latter was also apparent in several ray-tracing models. The combination of these in vivo results and ray-tracing simulations indicated that patients with negative dysphotopsia had a temporal-rotated eye, which confirmed the hypothesized relation between negative dysphotopsia and an increased angle κ.

Conclusions: Patients with negative dysphotopsia had a smaller pupil and an increased angle κ, which made them more susceptible to experiencing a shadow in the temporal visual field.

J Cataract Refract Surg 2020; 46:1007–1015 Copyright © 2020 The Author(s). Published by Wolters Kluwer Health, Inc. on behalf of ASCRS and ESCRS

Cataract, the clouding of the crystalline lens inside of the eye, is one of the principal causes of visual impairment, and it is generally treated by replacing that lens with an artificial intraocular lens (IOL).[1] Although cataract surgery has a very low rate of intraoperative and postoperative complications, recent studies have revealed that up to 19% of the patients experience an unwanted visual complaint known as negative dysphotopsia directly after cataract surgery, which persists for more than a year in 3.2% of these patients.[2,3] Because the cataract surgery rate is high, estimated at 4000 per million people in 2020, this would result in roughly 6 million people being affected by negative dysphotopsia each year, of which at least 1 million will have persistent complaints.[A]

Negative dysphotopsia is commonly described as a shadow in or missing part of the peripheral temporal visual field.[4–7] It has been reported with a wide variety of IOL types and is generally more pronounced under photopic conditions.[6,7] Although the reported incidence of negative dysphotopsia, when actively surveyed, is quite high, the severity of the complaints often reduces over time, in many cases resolving fully. However, for the 3.2% of the patients who are still experiencing negative dysphotopsia 1 year postoperatively, the chance of spontaneous reduction or resolution of the complaints is minimal.[3]

Although clinical evaluations revealed no evident abnormalities in patients with negative dysphotopsia, for

example, no abnormalities in IOL position, optical ray-tracing simulations revealed various methods to induce a shadow in the peripheral visual field.[5,7–9] One of the main hypothesized mechanisms is the occurrence of an un-illuminated area on the peripheral nasal retina that is experienced as a shadow in the temporal visual field.[8,10] Such an unilluminated retina, for example, could be the result of a discontinuity in illumination between light that is refracted by the optic and light that misses the optic and passes through the gap between the iris and IOL (the iris–IOL gap).[8,10]

Multiple factors that potentially affect this discontinuity in retinal illumination have also been investigated using these same simulations. For example, an evaluation of the pupil size showed that the shadow is more profound with small pupils, which was also reported in clinical evaluations.[7,8] In addition, a relationship was found between the discontinuity in retinal illumination and a positive angle κ, the angle between the pupillary axis and the visual axis.[8,11] At a larger angle, more light rays would be able to pass between the IOL and iris, increasing the experienced discontinuity in retinal illumination. Furthermore, the optic diameter, edge design, aspheric surface design, material, and alignment of the IOL have been proposed to affect the occurrence and severity of negative dysphotopsia, although their effect is likely to be minor.[8] Other studies identified various optical effects caused by the capsular bag that could lead to negative dysphotopsia. These optical effects include the lack of blockage of peripheral light rays by a nontranslucent capsular bag, a reduction in peripheral transmitted light due to the capsular bag, and visible arcs and bands caused by the capsulorhexis–IOL interaction.[5,8,9]

Although many of these mechanisms could lead to negative dysphotopsia, no definite conclusion on its origin has been made. Nevertheless, these proposed mechanisms have formed the basis for various preventive approaches, such as performing a primary reverse optic capture or implanting the IOL with a horizontal orientation of the haptics, and many different treatments of negative dysphotopsia.[5,6,8,10,12–21] Some of these treatments were successful in small groups of patients, but none gave full resolution in all patients. This lack of a definite strategy to resolve negative dysphotopsia is mainly due to the lack of clinical data that could discriminate between the different proposed origins of negative dysphotopsia because this would give a clear indication of more successful treatment strategies.

In this study, we aimed to provide quantitative clinical data of pseudophakic eyes with and without negative dysphotopsia to gain a better understanding of the anatomical characteristics that are associated with negative dysphotopsia. First, the anterior segment configuration, evaluated by anterior segment tomography and biometry, was analyzed because small geometrical differences could result in significant differences in peripheral vision and, therefore, have a relation to negative dysphotopsia. Second, the ocular wavefront aberrations were evaluated along the horizontal meridian to quantify potential objective refractive differences in the peripheral vision. Finally, the relation between differences in anterior segment configuration and peripheral ocular aberrations was studied using ray-tracing simulations to relate the effects of the various proposed origins of negative dysphotopsia to the clinical data.

METHODS

Patients with pseudophakic eyes with and without clinically reported negative dysphotopsia were studied at the Leiden University Medical Center. Patients were excluded if they had any additional ocular surgery, such as laser in situ keratomileusis, which would severely modify the optical properties of the eye. The study was performed to conform to the tenets of the Declaration of Helsinki and approved by the local Medical Ethics Committee (CCMO-registry number: NL58358.058.16).

In total, 57 pseudophakic eyes of 27 patients with negative dysphotopsia and 30 pseudophakic control subjects were prospectively included between November 2016 and May 2019. The pseudophakic control subjects were included from 3 centers, and the patients with negative dysphotopsia were referred from 17 different centers after an otherwise uneventful cataract surgery. For all referred patients with negative dysphotopsia, the diagnosis was confirmed before inclusion. The criteria for this diagnosis consisted of a patient-reported shadow or dark region in the temporal peripheral visual field that occurred after an otherwise uneventful cataract surgery, no evident cause of this visual complaint, and no clear anomalies in IOL positioning on slitlamp examination. Although the pseudophakic control subjects had not reported any complaints during the regular follow-up after cataract surgery, 4 control subjects reported the presence of a temporal shadow when they were actively screened for negative dysphotopsia at the beginning of the study.[2] These 4 subjects and 1 more control subject with a raised suspicion of staphyloma after inclusion were excluded from further analysis.

Study procedures were performed after the patients provided written informed consent. The study procedures included anterior segment tomography, ocular biometry, and peripheral aberrometry for 1 eye (Figure 1). The baseline equality of both resulting groups of patients was assessed by comparing the sex and age of the patients and the laterality, keratometry, axial length, and implanted IOL type of the studied eye.

Anterior Segment Tomography and Biometry

The combined optical effect of the central 8.0 mm of the anterior and posterior corneal surfaces was evaluated with the Pentacam anterior segment tomographer (software version 1.20r41, OCULUS, Optikgeräte GmbH) in terms of total corneal wavefront, expressed in Zernike coefficients using the Pentacam's built-in software.[B] To limit the number of tested metrics, only the Zernike coefficients with a strong effect on the variation along the horizontal meridian, being $Z(1,1)$, $Z(2,0)$, $Z(2,2)$, and $Z(3,1)$, were selected for analysis.

The internal anterior chamber depth (ACD), horizontal decentration of the pupil center with respect to the corneal vertex, and the pupil diameter were obtained from tomography. Because it has been reported that the automated ACD measurement might fail in pseudophakic eyes, the ACDs were measured manually for each eye on 3 different Scheimpflug images and averaged.[22] The horizontal decentration of the pupil center with respect to the visual axis was also measured with the LENSTAR LS900 biometer (Haag-Streit AG), together with the pupil diameter, keratometry, and axial length. Based on the rationale that a larger angle κ results in a temporal rotation of the eye, the tilt of the iris was calculated by fitting a 3 D plane through the central 6.0 mm of the iris surface as measured by the Scheimpflug tomographer using a custom-written program in Python 3.6.
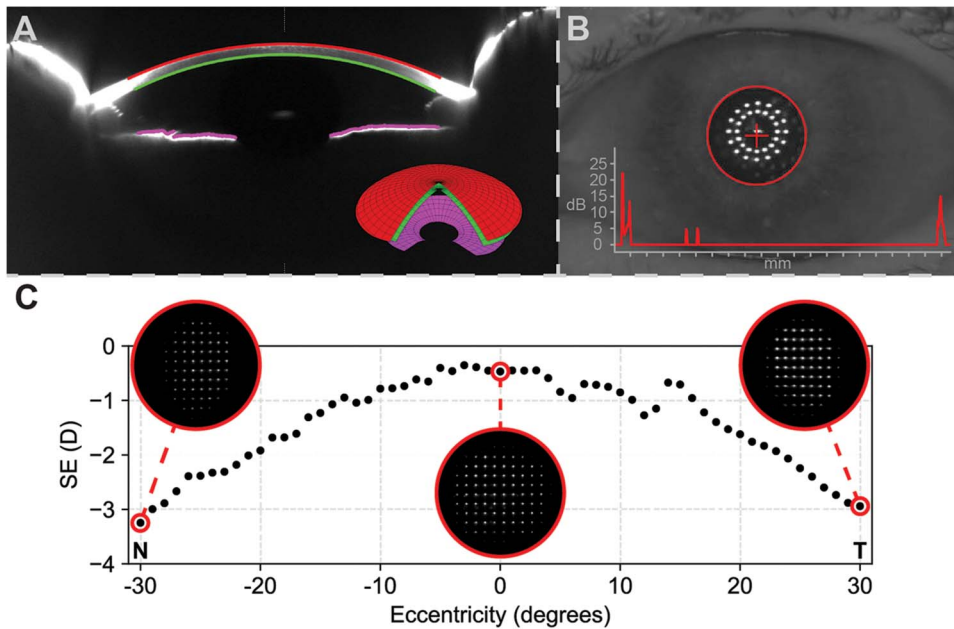
Figure 1. Overview of the performed clinical measurements. *A*: Anterior segment tomography showing the measured anterior (*red*) and posterior (*green*) corneal surfaces from which the corneal wavefront was calculated. In addition, the measured iris (*pink*) from which the iris tilt was calculated is shown. The inset shows the 3D model of the anterior segment, as obtained from the Pentacam. *B*: Biometry analysis showing the location of the pupil center with respect to the visual axis, and the biometry result as inset. *C*: The peripheral ocular aberrations, expressed as spherical equivalent (SE) of refraction in diopters (D), along the horizontal meridian up. The insets show the Hartmann-Slack images from which the refraction is calculated. At around 15 degrees eccentricity in the temporal visual field (T), a distortion that is not apparent on the nasal (N) side is visible. This distortion is caused by the reflection from the optic nerve head.

Peripheral Ocular Aberrations

Peripheral ocular aberrations along the horizontal meridian were measured using the VPR peripheral aberrometer (vOPTICA) as described by Jaeken et al.[23] Earlier studies with this technique showed that emmetropic eyes are relatively myopic at peripheral eccentricities and that pseudophakic eyes have stronger peripheral aberrations than those of phakic eyes.[24,25] The aberrometer quantifies the ocular aberrations up to 30 degrees eccentricity with a 1-degree step size using Hartmann-Shack wavefront sensor integrated in a rotating arm. The patient was instructed to look at a fixation target while the arm rotates, and the Hartmann-Shack images are acquired. Four measurements were performed per eccentricity, expressed in Zernike terms over the central 3.0 mm, and averaged. Each individual measurement takes about 2 seconds to complete. When the observer noted erroneous or missing results for certain eccentricities during the measurement, such as because of blinking, an additional measurement was performed. With the instructions, evaluations, and optional additional measurements, a full peripheral aberrometry measurement took on average 5 minutes per patient.

The aberration profiles were converted to spherical equivalent (SE, also known as power vector M) of refraction, astigmatism (also known as power vector J), and spherical aberration.[26] From the aberration profiles, the SE of refraction, astigmatism, and spherical aberration as measured for central vision and for peripheral vision at 30 degrees nasal and temporal visual field eccentricities were selected for statistical analysis. At 30 degrees eccentricity, the refraction relative to the central refraction was used for SE of refraction and astigmatism to correct for an intended offset in central refraction.[25]

Ray-Tracing Simulations

Ray-tracing simulations were performed to assess the relation between the peripheral ocular aberrations and various anterior segment configurations with a potential relation to negative dysphotopsia. A geometrical eye model was created in Zemax OpticStudio 18.9 (Zemax, LCC), and aberrations at 543 nm were calculated up to 30 degrees eccentricity with a 1-degree step size. Actual pupil size was adjusted to obtain a 3.0 mm apparent pupil size to match the peripheral ocular aberration measurements. The calculated aberrations were subsequently converted into SE of

refraction.[26,27] All simulations and analyses were automated using Python 3.6 and the PyZDDE library.[C]

The eye model was based on the wide-angle schematic eye model proposed by Escudero-Sanz and Navarro.[28] For accurate use in the evaluation of negative dysphotopsia, 2 adjustments were made to this model. First, the iris was moved 0.5 mm forward and given a thickness of 0.5 mm. Second, the crystalline lens was replaced by a simple IOL, placed 0.5 mm behind the posterior iris. The IOL had a refractive index of 1.47 and a thickness of 1.0 mm. The anterior radius of curvature, anterior conic constant, and posterior radius of curvature were chosen such that to match the central ocular aberrations of the phakic eye model of Escudero-Sanz and Navarro. This resulted in an IOL with an anterior radius of curvature of 19.5 mm, an anterior conic constant of −13.7 mm, a posterior radius of curvature of −11.2 mm, and an in situ paraxial power of 18.5 diopters (D).[8]

The variations in anterior segment configurations that were analyzed included IOL positioning, horizontal iris and IOL tilt, and an increase in angle κ. Two modifications in IOL positioning were evaluated: a 0.4 mm increase in axial distance between the iris and IOL, which would increase the iris–IOL gap, and a 1.0 mm temporal decentration of the IOL, which would increase the iris–IOL gap nasally. Because a temporal tilt or either the iris or both the iris and IOL would allow for easier passage of light through the nasal iris–IOL gap, both were evaluated. To this end, a tilt of 5.0 degrees temporally was induced in either the iris or both the iris and IOL. Finally, because a larger angle κ would result in an outward rotation of the eye with respect to the visual axis, and therefore in easier passage of light through the nasal iris–IOL gap, an angle κ of 5.0 degrees was induced and evaluated. This angle κ was created by adding 5.0 degrees to the incident angle. Because the IOL design is one of the potential factors of influence, these simulations were also performed using the pseudophakic eye models of Holladay and Simpson, with both acrylic and silicone IOLs.[8]

Statistical Analyses

All statistical analyses were performed with the presence of negative dysphotopsia as dependent or grouping variable. First, the baseline characteristics were compared between both groups. Second, the relation between negative dysphotopsia and the total

corneal wavefront, expressed in Zernike coefficients, was assessed using a logistic regression analysis. Third, all evaluated anterior segment configurations were compared using independent samples t tests. Finally, the central and peripheral ocular aberrations were compared using Mann-Whitney U tests. The statistical analyses were performed using SPSS Statistics 23 (IBM Corp.), except for the ocular aberrations, which were analyzed in Python 3.6 using the SciPy library version 1.1.0.[D] An α of 0.05 was set as critical value for significance for every test. Multiple testing correction was not applied because many of the tested parameters were geometrically correlated with each other.

RESULTS

In the baseline comparison, the group of patients with negative dysphotopsia had a higher percentage of women than that in the pseudophakic group ($P < .01$), with 24 out of 27 patients (88.9%) and 12 out of 25 controls (48.0%) being female. Furthermore, the pseudophakic control subjects had, on average, slightly longer eyes ($P = .02$). All other baseline parameters were comparable between both groups (Table 1). Some patients and control subjects were excluded from one of the performed analyses because of missing or erroneous data (Figure 2).

A wider variety of IOL types were seen in patients with negative dysphotopsia than that in pseudophakic group. In patients with negative dysphotopsia, a total of 10 different types of IOLs were implanted. Most of this group (14 subjects [51.9%]) had TECNIS ZCB00 IOLs (Johnson & Johnson Vision) implanted. In the pseudophakic group, 2 types of IOLs were implanted: the TECNIS ZCB00 IOL (19 subjects [76.0%]) and the Quadrimax IOL (Ophtec) (6 subjects [24.0%]). All IOLs were implanted within the capsular bag. For 1 patient with negative dysphotopsia, the capsulorhexis did not completely cover the IOL in the temporal inferior quadrant.

Corneal Wavefront

The total corneal wavefront along the horizontal meridian was similar for patients with negative dysphotopsia and pseudophakic control subjects, with equal distributions for all 4 evaluated Zernike coefficients in both groups (Figure 3).

In addition, the logistic regression analysis showed no significant relationship between the coefficients and the presence of negative dysphotopsia, with all P values being .09 or higher (Figure 3).

Anterior Chamber Depth

The ACDs of patients with negative dysphotopsia and pseudophakic control subjects were similar, with the mean ACDs of 4.17 mm (SD 0.38) and 4.30 mm (0.26), respectively ($P = .184$) (Figure 4, A).

Iris Tilt

The mean horizontal tilt of the iris was significantly larger for patients with negative dysphotopsia than that for pseudophakic control subjects ($P < .01$) (Figure 4, B), with the mean tilts of 6.3 degrees (1.4), and 4.6 degrees (1.5), respectively. The larger positive tilt indicates a more temporally tilted iris in patients with negative dysphotopsia.

Pupil Decentration

The pupil center of patients with negative dysphotopsia was located significantly more temporally than that in pseudophakic control subjects on both anterior segment tomography and ocular biometry. On anterior segment tomography, the mean horizontal distance from the corneal vertex was 0.17 mm (0.14) and 0.01 mm (0.16) for patients with negative dysphotopsia and pseudophakic control subjects, respectively ($P < .01$) (Figure 4, C). Similar results were obtained from biometry, with the mean decentrations of 0.19 mm (0.21) and 0.03 mm (0.16) from the visual axis, respectively ($P < .01$) (Figure 4, C).

Pupil Diameter

Patients with negative dysphotopsia had a significant smaller pupil than that in the pseudophakic control subjects on both anterior segment tomography and ocular biometry. On tomography, the mean pupil diameters were 2.4 mm (0.4) and 2.7 mm (0.4) for patients with negative dysphotopsia and pseudophakic control subjects, respectively

Table 1. Demographics of both groups.			
Characteristic	**Patients with ND**	**Pseudophakic Control Subjects**	**P Value**
Patients (n)	27	25	
Female sex (%)	88.9	48.0	<.01*
Laterality, right (%)	40.7	48.0	.78
Age (y), mean ± SD	65.9 ± 8.1	69.0 ± 8.2	.18
Km, corneal (D), mean ± SD	44.1 ± 1.4	44.1 ± 1.3	0.90
Astigmatism, corneal (D), mean ± SD	−1.0 ± 0.8	−0.8 ± 0.5	.49
Axial length (mm), mean ± SD	23.3 ± 1.1	24.2 ± 1.5	.02*
Implanted IOL type (n)	ZCB00 (14)	ZCB00 (19)	
	SN60WF (3)	Quadrimax (6)	
	Quadrimax (2)		
	iSert 251 (2)		
	Other[†] (6)		

IOL = intraocular lens; Km = maximum keratometry; ND = negative dysphotopsia
*Statistically significant.
[†]CT LUCIA (1), Fine Vision (1), MI60 (1), MX60 (1), MPlus (1) and SA60AT (1).
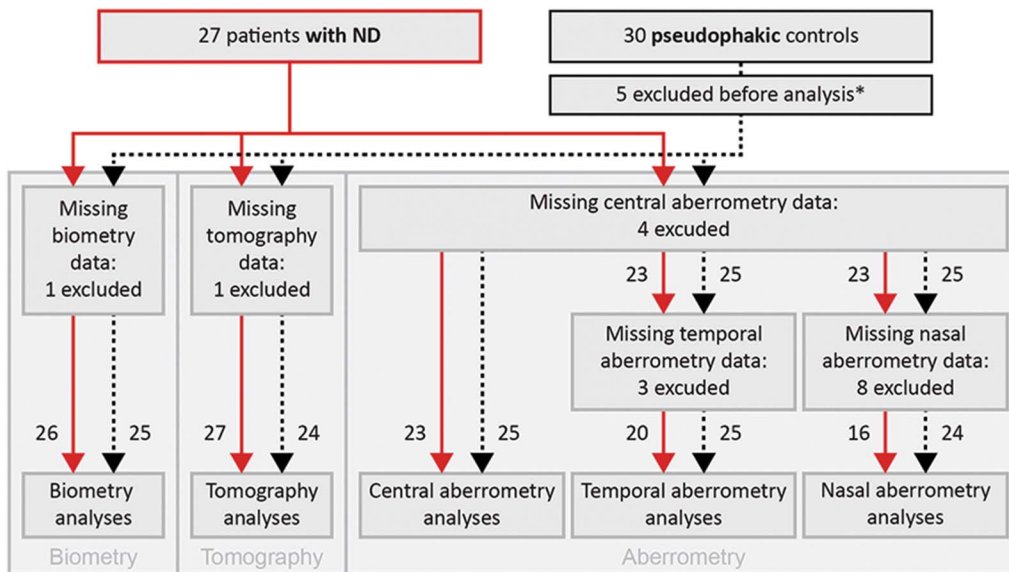
Figure 2. A flowchart depicting the amount of patients included in various analyses. Patients with negative dysphotopsia are represented by the *red continuous lines* and pseudophakic control subjects by the *black dashed lines*. Next to each line, the number of patients is stated. *Five pseudophakic control subjects were excluded from all analyses, 4 because of a reported presence of negative dysphotopsia during the study measurements, and 1 because of a raised suspicion of staphyloma after inclusion (ND = negative dysphotopsia).

($P < .01$) (Figure 4, D). These diameters were 3.7 mm (0.6) and 4.1 mm (0.7) on biometry, respectively ($P = .03$) (Figure 4, D).

Peripheral Ocular Aberrations

In general, peripheral aberrometry showed the earlier described trend of a decreasing SE of refraction of up to −2.00 D at 30 degrees eccentricity, whereas the astigmatism increased up to 3.00 D (Table 2 and Figure 5, A and B).[25] Centrally, there was no difference between both groups in SE of refraction, astigmatism, and spherical aberrations. Peripherally, however, a difference between patients with and without negative dysphotopsia was noted, the reason being a clear asymmetry between relative SE of refraction at nasal and temporal eccentricities visible in patients with negative dysphotopsia but not in pseudophakic control subjects (Figure 5, A).

At temporal visual field eccentricities, where negative dysphotopsia was manifested, the median relative SEs of refraction of −1.5 D and −1.4 D were measured for patients with negative dysphotopsia and pseudophakic control subjects, respectively ($P = .9$) (Table 2). However, for nasal eccentricities, a statistically significant difference in relative SE of refraction was found, with −3.6 D for patients with negative dysphotopsia and −1.8 D for pseudophakic control subjects ($P = .04$) (Table 2). The astigmatism as a function of horizontal visual field showed a comparable, although not statistically different, course between both groups (Table 2 and Figure 5, B). The spherical aberration was relatively constant as a function of horizontal visual field and did not show a difference between patients with or without negative dysphotopsia (Table 2 and Figure 5, C).

Ray-Tracing Simulations

The ray-tracing simulations using the pseudophakic eye model of Escudero-Sanz and Navarro without additional modifications showed a symmetric decrease of the SE of refraction in the peripheral visual field, similar to the in vivo aberrometry of the pseudophakic control subjects (Figure 6, A and G).

Increasing the axial distance between the iris and IOL by 0.4 mm resulted in an overall increase in SE of refraction of approximately 1 D (Figure 6, B and G). A temporally decentered IOL resulted in an asymmetric change in SE of refraction, where a more negative SE of refraction was seen at nasal eccentricities than at temporal eccentricities (Figure 6, C and G).

Tilting solely the iris had almost no effect on the resulting aberration profile (Figure 6, D and G). A combined temporal tilt of the iris and the IOL, however, resulted in an asymmetric change similar to the change induced by a temporal decentration of the IOL, with a more negative SE of refraction at nasal eccentricities (Figure 6, E and G).

Inducing a positive degree angle κ, which is equivalent to a temporal rotation of the eye, also resulted in an asymmetric peripheral aberration profile. Similar to the simulation with
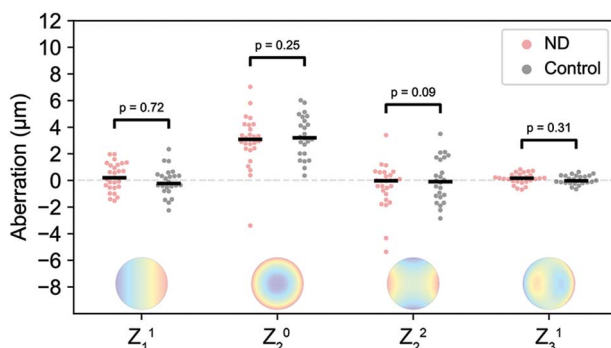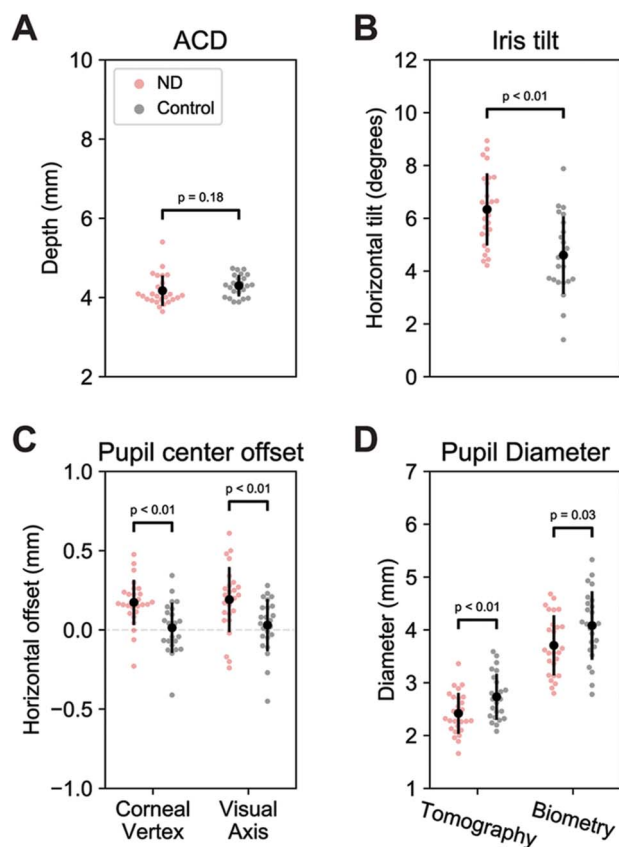

Figure 3. Distribution of the total corneal wavefront, expressed in the Zernike coefficients with a major influence on deviations along the horizontal meridian. No clear differences are observed between negative dysphotopsia (*red dots*) and pseudophakic controls (*gray dots*). The horizontal lines depict the medians per group (ND = negative dysphotopsia).

Figure 4. Anterior chamber configurations for patients with negative dysphotopsia (*red dots*) and control subjects (*gray dots*), showing that patients with negative dysphotopsia, on average, have a temporally shifted and smaller pupil and a more tilted iris. *Black dots* display the means and the *vertical lines* the SD. *A*: The anterior chamber depth (ACD). *B*: The horizontal iris tilt. A positive tilt indicates a temporal tilt. *C*: Horizontal decentration of the pupil center with respect to the corneal vertex and the visual axis. A positive decentration indicates a temporal shift of the pupil. *D*: The pupil diameter as measured by tomography and biometry (ND = negative dysphotopsia).

a temporal decentration of the IOL, a stronger decrease in SE of refraction was observed at nasal eccentricities (Figure 6, F and G). The amount of asymmetry (0.7 D) was, however, smaller compared with a decentration of the IOL (1.6 D) or a combined tilt of the iris and the IOL (1.2 D, Figure 6, G). The simulations using the two eye models described by Holladay and Simpson provided similar results, although with differences in magnitude of both the peripheral aberrations and their asymmetric development to higher eccentricities because of the differences in the eye geometry and IOL properties (Figure 7, Supplementary Digital Content, available at http://links.lww.com/JRS/A65).[8]

DISCUSSION

Since the initial description of negative dysphotopsia in 2000, various etiological theories have been proposed.[4,5,7–9] These theories have, however, not yet been confirmed or disproved because of a lack of clinical data on the anterior chamber configuration in negative dysphotopsia. In this study, we presented an elaborate combination of quantitative geometrical and optical measurements in pseudophakic eyes

with and without negative dysphotopsia to provide clinical insights into anatomical differences that are associated with negative dysphotopsia.

The group of patients with negative dysphotopsia was comparable with the group of pseudophakic control subjects, except for a higher percentage of women, a shorter axial length, and a larger variation in IOL types (Table 1). Both the higher percentage of women and the shorter axial length have been reported earlier for patients with negative dysphotopsia and might be related to each other.[2,13,29] In addition, a wide variety of IOL types was implanted in the studied group of patients with negative dysphotopsia, confirming the earlier reports that negative dysphotopsia is not just occurring with certain IOL types.[15] Because the pseudophakic control subjects were included from a limited number of clinics, a smaller variety of IOLS were implanted in this cohort. Although this is a limitation of the study design, we do not expect this to influence the results because the outcome measurements, such as pupil diameter, are relatively invariant of IOL design, and the IOL types of the control group are also present in the negative dysphotopsia group.

Because the cornea is the strongest refractive element of the eye, any distinct difference in corneal shape could result in severe visual complaints, both centrally and peripherally. The main components of the total corneal wavefront along the horizontal meridian were comparable between patients with and without negative dysphotopsia (Figure 3), rendering it unlikely that negative dysphotopsia originates from an abnormal corneal shape. Although the location of the corneal incision of the cataract surgery could affect the peripheral aberrations, a direct causal relation with negative dysphotopsia is unlikely because no significant differences were observed in the total corneal wavefront.

Although anterior segment imaging showed no abnormalities in either the cornea or the ACD of patients with negative dysphotopsia, it revealed three significant differences in the iris configuration. First, a smaller pupil diameter was found in patients with negative dysphotopsia, which is in line with the theoretically demonstrated relationship between pupil size and negative dysphotopsia.[5,9] Second, the pupil centers of patients with negative dysphotopsia were more temporally located with respect to both the corneal vertex and the visual axis. This pupil decentration is probably related to the third difference, a significantly strongly tilted iris toward the temporal side with respect to the visual axis in patients with negative dysphotopsia. This stronger tilt indicates that, with respect to the visual axis, either the iris is tilted more temporally within the eye or the eye is rotated more temporally. Such a temporal rotation of the eye could be caused by a larger positive angle κ, which is one of the possible causes of negative dysphotopsia.[8,11,30] Although a correlation between angle κ and axial length has been reported, it cannot be the cause of the 1.5-degree increase in angle κ, because the 0.9 mm increase in axial length would correlate with less than a 0.5-degree increase in angle κ.[31,32]

Table 2. Peripheral aberrometry showed a significant difference in nasal relative spherical equivalent (SE) of refraction.

Parameter	Patients with ND			Pseudophakic Control Subjects			P Value
	Median	Q1*	Q3*	Median	Q1*	Q3*	
Central aberrations							
SE of refraction (D)	−0.73	−1.02	−0.44	−0.85	−2.50	−0.41	.64
Astigmatism (D)	0.38	0.26	0.57	0.44	0.24	0.71	.41
Sph. ab (µm)	0.001	−0.048	0.019	0.002	−0.016	0.021	.40
Nasal aberrations†							
Rel. SE of refraction (D)	−3.56	−4.29	−2.56	−1.75	−3.17	−0.91	**.04**
Rel. astigmatism (D)	3.04	2.04	4.05	2.43	1.89	2.91	.11
Sph. ab (µm)	−0.040	−0.132	0.020	−0.023	−0.046	−0.008	.59
Temporal aberrations†							
Rel. SE of refraction (D)	−1.52	−2.09	−0.64	−1.38	−2.44	−0.12	.90
Rel. astigmatism (D)	1.44	0.83	1.96	1.08	0.66	1.70	.43
Sph. ab (µm)	−0.022	−0.061	0.011	0.000	−0.044	0.022	.95

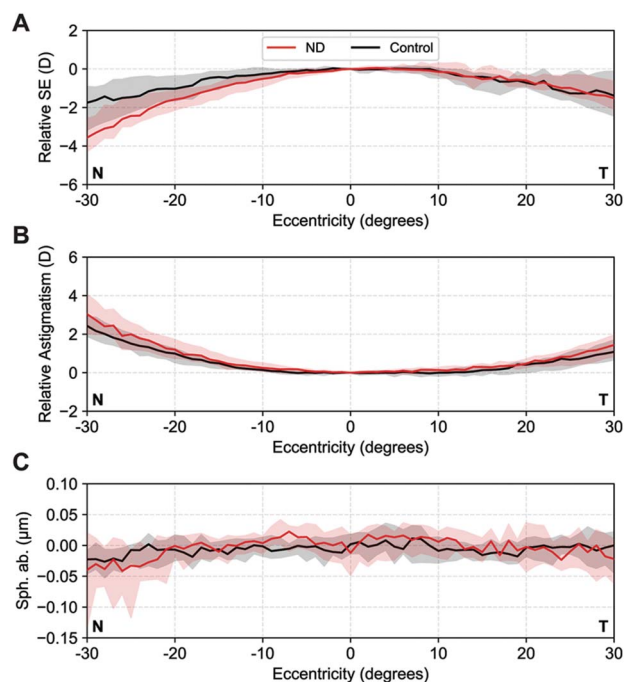ND = negative dysphotopsia; Rel. = relative; SE = spherical equivalent; Sph. ab = spherical aberration
*Q1 and Q3 are the 25th and 75th percentiles.
†Measured at 30 degrees visual field eccentricity. A significant difference in SE between patients with ND and pseudophakic controls is seen in the nasal peripheral visual field (P = .04).

Clear differences were also found in the peripheral ocular aberrations. Overall, patients with negative dysphotopsia show an asymmetric decrease in SE of refraction toward the nasal visual field, which results in a significant lower relative SE of refraction at 30 degrees. These peripheral aberration measurements would ideally have been performed at higher eccentricities because negative dysphotopsia is

Figure 5. *A*: Relative spherical equivalent (SE) of refraction in diopters (D). *B*: Relative astigmatism (D). *C*: Spherical aberration (µm) as a function of visual field eccentricity. Negative eccentricities are acquired at the nasal visual field (N). Patients with negative dysphotopsia (*red*) show a stronger decrease in SE of refraction at nasal eccentricities than control subjects (*black*). The median value at each eccentricity is indicated by the *solid line* and the interquartile range is depicted by the *shaded area* (ND = negative dysphotopsia).
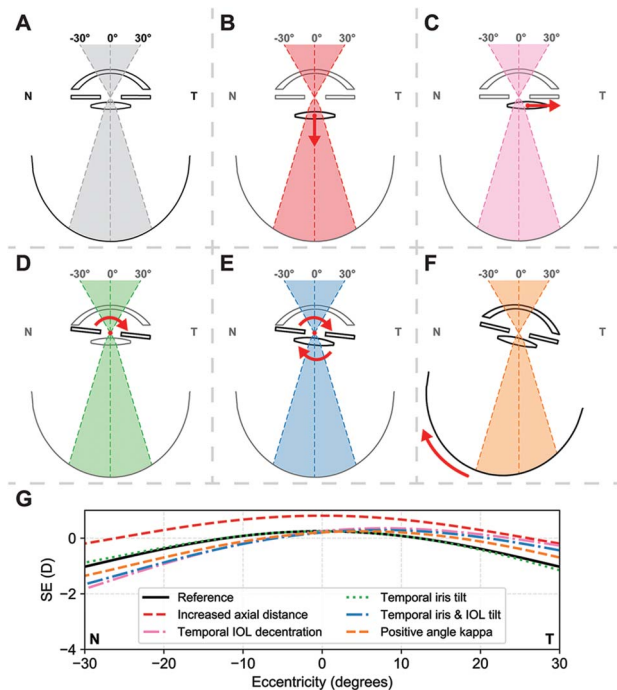
generally not apparent at 30 degrees. Unfortunately, there are currently no techniques available to assess the optical wavefronts at higher eccentricities because the quality of the Hartmann-Shack images deteriorates at the far peripheral field. Although the peripheral aberrations are partly affected by the slightly different axial lengths and implanted IOL types between both study groups, these differences are not likely to be causative of the observed asymmetry in the peripheral myopization. The relatively low eccentricities at which the aberrations were assessed in this study explain why no direct effect of negative dysphotopsia, such as a loss of signal, was observed in the temporal visual field. These measured differences in midperipheral eccentricities between both groups do, however, aid in the understanding of negative dysphotopsia because they provide a link to the ray-tracing simulations in which the effect of a difference in ocular geometry is evaluated.

The ray-tracing simulations showed that several of the tested potential factors of influence on the origin of negative dysphotopsia result in an asymmetric change in SE of refraction toward higher eccentricities, similar to patients with negative dysphotopsia. In particular, these asymmetries could be induced by a temporal decentration of the IOL, a combined temporal tilt of the iris and the IOL, and a temporal rotation of the eye with respect to the visual axis resulting from a positive angle κ (Figure 6, C, E and F). Because the clinical slitlamp evaluations revealed no evident abnormalities, a strong temporal decentration of the IOL is unlikely.[7] This confirms earlier ray-tracing studies that suggest a minor role of IOL decentration in the etiology of negative dysphotopsia.[8] Furthermore, because a tilt of solely the iris had only a very minor effect on the peripheral refraction (Figure 6, D), the observed asymmetric peripheral refraction in negative dysphotopsia is likely caused by either a combined tilt of the iris and IOL or from a rotation of the eye with respect to the visual axis. Although both these effects would result in the observed increased iris tilt in the subjects with negative dysphotopsia,

Figure 6. Ray-tracing analyses on the effect of several of the proposed origins of negative dysphotopsia on the peripheral ocular aberrations. *A–F*: Schematic representation of the tested conditions: *A*: reference model; *B*: an increased axial distance between the iris and IOL; *C*: temporal decentration of the IOL; *D*: temporal tilt of the iris; *E*: combined temporal tilt of the iris and IOL; and *F*: positive angle κ. *G*: The simulations for the decentered IOL, a tilted iris and an IOL, and an increased angle κ show a similar asymmetry in the peripheral spherical equivalent (SE) of refraction as observed in patients with negative dysphotopsia.

location of the IOL with respect to the iris need to be personalized as well.

These, fully personalized, simulations could also aid in the design of an effective treatment of negative dysphotopsia, which takes the increased angle κ into account. Furthermore, they might provide insights into the suboptimal results of treatments such as laser capsulotomy, implanting a piggyback IOL, or exchanging the IOL.[10,16–19] Any of these treatments can change the configuration of the anterior eye chamber and, thereby, potentially reduce the chance of light rays passing through the iris–IOL gap.

Overall, this study identified several anatomical differences between patients with and without negative dysphotopsia, which provide a basis for further research. There are, however, some study limitations that should be considered while interpreting these results. Ideally, the study should have been a prospective cohort study in which the patients were included before cataract surgery. This would also result in a more uniform distribution of IOL types and allow for the inclusion of intraoperative data, such as the location of the corneal incision, in the analysis. However, given the low incidence of persistent negative dysphotopsia of approximately 3%, this is not feasible.[3] Furthermore, the group differences in axial length and sex could have introduced a bias in the measurements, but this could also be a predisposition to negative dysphotopsia because other studies also observed a similar difference.[2,13] In addition, other studies reported a higher incidence of negative dysphotopsia in the left eye, which was not present in our study population.[3,4,13] Finally, the eye models for the ray-tracing analyses were not fully personalized to completely match the eyes of individual patients with negative dysphotopsia, which would allow for a more in-depth analysis of the optical interplay between the anatomy of the eye and the IOL.

This study provides, despite these limitations, valuable insights into the etiology of negative dysphotopsia based on clinically measured data, which yields a base for further research on the origin, management, and prevention of negative dysphotopsia. The measurement and simulation results show that the iris and IOL plane are rotated temporally with respect to the visual axis, which corresponds to the role of an increased angle κ in earlier ray-tracing studies on the etiology of negative dysphotopsia. Although these anatomical differences cannot be modified easily, IOL designs can be optimized to mitigate the effect of differences, which could benefit the treatment of negative dysphotopsia or might even prevent it from occurring. Furthermore, the presented anatomical differences might be able to preoperatively select patients who might have a high risk of negative dysphotopsia after cataract surgery, but larger, prospective studies are needed to develop and validate this. In conclusion, this study presents the first clinical insights into anatomical differences between patients with and without negative dysphotopsia, which both substantiate one of the leading theories behind the etiology of negative dysphotopsia and provides a basis for further research.

only a rotation of the complete eye would result in the increased decentration of the pupil center.

Earlier ray-tracing stimulations have shown a clear relationship between a larger positive angle κ and discontinuity in retinal illumination.[8] Furthermore, it has been suggested that such a temporal rotation of the eye with respect to the visual axis would additionally result in a more anterior position of the functional nasal retina (Figure 6, F), thereby increasing the perception of negative dysphotopsia.[5,6] Although the combined analysis of the data of this study provides a strong support for an increased angle κ as one of the main contributing factors to negative dysphotopsia, other factors can play an additional role in the origin of negative dysphotopsia. The potential role of neural adaptation, for example, requires a different set of examinations to gain insights into its potential contribution to the spontaneous resolution of the complaints in some patients.[33,34] The results of this study can, however, explain the reported preventative effect of implanting IOLs with the haptics oriented horizontally because this orientation could put the haptics in the path of rays of light passing through the gap between the iris and IOL.[12] Ray-tracing simulations using fully personalized eye models could aid to identify these factors.[10,18] For a clinically relevant assessment using these analyses, however, the orientation of the iris and the

WHAT WAS KNOWN

- Negative dysphotopsia can theoretically be caused by many factors such as a smaller pupil size, a larger angle κ, or an optical effect of the capsular bag.

WHAT THIS PAPER ADDS

- Clinical data substantiating the role of a smaller pupil size and a larger angle κ in the etiology of negative dysphotopsia were obtained.

REFERENCES

1. Pascolini D, Mariotti SP. Global estimates of visual impairment: 2010. Br J Ophthalmol 2012;96:614–618
2. Makhotkina NY, Nijkamp MD, Berendschot T, van den Borne B, Nuijts R. Effect of active evaluation on the detection of negative dysphotopsia after sequential cataract surgery: discrepancy between incidences of unsolicited and solicited complaints. Acta Ophthalmol 2018;96:81–87
3. Osher RH. Negative dysphotopsia: long-term study and possible explanation for transient symptoms. J Cataract Refract Surg 2008;34:1699–1707
4. Davison JA. Positive and negative dysphotopsia in patients with acrylic intraocular lenses. J Cataract Refract Surg 2000;26:1346–1355
5. Holladay JT, Zhao H, Reisin CR. Negative dysphotopsia: the enigmatic penumbra. J Cataract Refract Surg 2012;38:1251–1265
6. Henderson BA, Geneva II. Negative dysphotopsia: a perfect storm. J Cataract Refract Surg 2015;41:2291–2312
7. Masket S, Fram NR. Pseudophakic negative dysphotopsia: surgical management and new theory of etiology. J Cataract Refract Surg 2011;37:1199–1207
8. Holladay JT, Simpson MJ. Negative dysphotopsia: causes and rationale for prevention and treatment. J Cataract Refract Surg 2017;43:263–275
9. Hong X, Liu Y, Karakelle M, Masket S, Fram NR. Ray-tracing optical modeling of negative dysphotopsia. J Biomed Opt 2011;16:125001
10. Erie JC, Simpson MJ, Bandhauer MH. Effect of a sulcus-fixated piggyback intraocular lens on negative dysphotopsia: ray-tracing analysis. J Cataract Refract Surg 2019;45:443–450
11. Basmak H, Sahin A, Yildirim N, Papakostas TD, Kanellopoulos AJ. Measurement of angle kappa with synoptophore and Orbscan II in a normal population. J Refract Surg 2007;23:456–460
12. Henderson BA, Yi DH, Constantine JB, Geneva II. New preventative approach for negative dysphotopsia. J Cataract Refract Surg 2016;42:1449–1455
13. Masket S, Fram NR, Cho A, Park I, Pham D. Surgical management of negative dysphotopsia. J Cataract Refract Surg 2018;44:6–16
14. Simpson MJ. Mini-review: far peripheral vision. Vis Res 2017;140:96–105
15. Geneva II, Henderson BA. The complexities of negative dysphotopsia. Asia Pac J Ophthalmol (Phila) 2017;6:364–371
16. Cooke DL, Kasko S, Platt LO. Resolution of negative dysphotopsia after laser anterior capsulotomy. J Cataract Refract Surg 2013;39:1107–1109
17. Folden DV. Neodymium:YAG laser anterior capsulectomy: surgical option in the management of negative dysphotopsia. J Cataract Refract Surg 2013;39:1110–1115
18. Makhotkina NY, Dugrain V, Purchase D, Berendschot TTJM, Nuijts RMMA. Effect of supplementary implantation of a sulcus-fixated intraocular lens in patients with negative dysphotopsia. J Cataract Refract Surg 2018;44:209–218
19. Weinstein A. Surgical experience with pseudophakic negative dysphotopsia. J Cataract Refract Surg 2012;38:561; author reply 561
20. Burke TR, Benjamin L. Sulcus-fixated intraocular lens implantation for the management of negative dysphotopsia. J Cataract Refract Surg 2014;40:1469–1472

21. Vamosi P, Csakany B, Nemeth J. Intraocular lens exchange in patients with negative dysphotopsia symptoms. J Cataract Refract Surg 2010;36:418–424
22. Savini G, Olsen T, Carbonara C, Pazzaglia S, Barboni P, Carbonelli M, Hoffer KJ. Anterior chamber depth measurement in pseudophakic eyes: a comparison of Pentacam and ultrasound. J Refract Surg 2010;26:341–347
23. Jaeken B, Lundström L, Artal P. Fast scanning peripheral wave-front sensor for the human eye. Opt Express 2011;19:7903–7913
24. Jaeken B, Artal P. Optical quality of emmetropic and myopic eyes in the periphery measured with high-angular resolution. Invest Ophthalmol Vis Sci 2012;53:3405–3413
25. Jaeken B, Mirabet S, Marin JM, Artal P. Comparison of the optical image quality in the periphery of phakic and pseudophakic eyes. Invest Ophthalmol Vis Sci 2013;54:3594–3599
26. Thibos LN, Wheeler W, Horner D. Power vectors: an application of Fourier analysis to the description and statistical analysis of refractive error. Optom Vis Sci 1997;74:367–375
27. Iskander DR, Davis BA, Collins MJ, Franklin R. Objective refraction from monochromatic wavefront aberrations via Zernike power polynomials. Ophthalmic Physiol Opt 2007;27:245–255
28. Escudero-Sanz I, Navarro R. Off-axis aberrations of a wide-angle schematic eye model. J Opt Soc Am A Opt Image Sci Vis 1999;16:1881–1891
29. Jongenelen S, Rozema JJ, Tassignon MJ; Evicr.net, Project Gullstrand Study Group. Distribution of the crystalline lens power in vivo as a function of age. Invest Ophthalmol Vis Sci 2015;56:7029–7035
30. Atchison DA, Smith G. Chapter 3: The Pupil. In: Optics of the Human Eye. Oxford, United Kingdom: Butterworth-Heinemann; 2000:35–36
31. Arba Mosquera S, Verma S, McAlinden C. Centration axis in refractive surgery. Eye Vis (Lond) 2015;2:4
32. Choi SR, Kim US. The correlation between angle kappa and ocular biometry in Koreans. Korean J Ophthalmol 2013;27:421–424
33. Masket S, Rupnik Z, Fram NR. Neuroadaptive changes in negative dysphotopsia during contralateral eye occlusion. J Cataract Refract Surg 2019;45:242–243
34. Wenzel M, Langenbucher A, Eppig T. Causes, diagnosis and therapy of negative dysphotopsia [in German]. Klin Monbl Augenheilkd 2019;236:767–776

OTHER CITED MATERIALS

A. World Health Organization. Programme for the Prevention of Blindness and Deafness. Global Initiative for the Elimination of Avoidable Blindness. 2000
B. American National Standards Institute. ANSI Z80.28-2010: Methods for Reporting Optical Aberrations of Eyes. 2010
C. Sinharoy I, Holloway C, Nummela V, Stuermer. indranilsinharoy/PyZDDE: Release version v2.0.3. 2016
D. Jones E, Oliphant T, Peterson P. SciPy: Open Source Scientific Tools for Python. 2001

First author:
Luc van Vught, BSc

Department of Ophthalmology, Leiden University Medical Center, the Netherlands